Grafted dinuclear zinc complexes for selective recognition of phosphatidylserine: Application to the capture of extracellular membrane microvesicles

Angéline Van der Heyden,[a], Phoulinh Chanthavong,[a] Eduardo Angles-Cano,[b] Hugues Bonnet,[a] Jerôme Dejeu,[a] Audrey Cras,[b] Christian Philouze,[a] Guy Serratrice,[a] Fatiha Zoubari El-Ghazouani,[c] Florence Toti,[c] Aurore Thibon-Pourret,[a] Catherine Belle,[a]**

[a] Université Grenoble-Alpes, CNRS, UMR 5250, Department of Molecular Chemistry (DCM), , 38000 Grenoble, France

[b] Université de Paris Cité, INSERM, Innovative Therapies in Haemostasis (IThEM), F-75006 Paris, France

[c] Université de Strasbourg-INSERM, UMR 1260, Centre de Recherche en Biomédecine (CRBS), 67084 Strasbourg, France

Keywords: zinc complexes, phosphatidylserine, surface-immobilized, microparticles

Abstract: Microvesicles (MVs) are key markers in human body fluids that reflect cellular activation related to diseases as thrombosis. These MVs display phosphatidylserine at the outer leaflet of their plasma membrane as specific recognition moieties. The work reported in this manuscript focuses on the development of an original method where MVs are captured by

bimetallic zinc complexes. A set of ligands have been synthetized based on a phenol spacer bearing in *para* position an amine group appended to a short or a longer alkyl chain (for grafting on surface) and bis(dipicolylamine) arms in *ortho* position (for zinc coordination). The corresponding dibridged zinc phenoxido and hydroxido complexes have been prepared in acetronitrile in presence of triethylamine and characterized by several spectroscopic techniques. The pH-driven interconversion studies for both complexes in H_2O:DMSO (70:30) evidence that at physiologic pH the main species are mono-bridged by the phenoxido spacer. An X-Ray structure obtained from complex **2** (based on the ligand with the amine group on the short chain) in aqueous medium confirms the presence of a mono-bridged complex. Then, the complexes have been used for interaction studies with short-chain phospholipids. Both have established the selective recognition of the anionic phosphatidylserine model versus zwitterionic phospholipids (in solution by ^{31}P NMR and after immobilization on solid support by surface plasmon resonance (SPR)). Moreover, both complexes have also demonstrated their ability to capture MVs isolated from human plasma. These complexes are thus promising candidates for MVs probing by a new approach based on coordination chemistry.

1. Introduction

Zinc-dipicolylamine (Zn-DPA) units (Scheme 1A) have long been identified as valuable tools for the recognition of anionic biomolecules such as biological phosphates [1] or phosphatidylserine (PS), the latter being a characteristic feature of the stimulated cells membrane.[2] PS has two distinct structural regions: 1) a polar anionic headgroup and 2) a hydrophobic tail group. (Scheme 1B). Usually, PS constitutes ≤ 10 % of the total phospholipid in the cell membrane phospholipids, which includes phosphatidylcholine (PC), phosphatidylethanolamine (PE), phosphatidylinositol,

etc. In resting cells, PS is confined to the internal side of the plasma membrane.[3] However, upon stimulation, or cell death, the phospholipid distribution is randomized, owing to the translocation of PS to the external leaflet of the cell membrane. In this context, dimetallic architectures with two appended Zn-DPA units associated to a bridging spacer leaving coordination sites free for anion binding, appear of particular interest for the enhanced and stable detection of PS.[4–6] Thus, the sensing of damaged or activated cells by targetting PS exposure has been widely exploited. Smith and coworkers' group, pioneer in the field, grafted various functional groups to the zinc complexes to enable fluorescence or NMR imaging and probed PS-enriched liposomes and PS-exposing cells.[7] The main applications were cell death imaging demonstrated in vitro in a variety of cell lineages [8–10] and in animal models of infection.[11] Beside cell death and apoptosis, it is now well demonstrated that the loss of membrane phospholipids asymmetry in response to a variety of stimuli also triggers the release of membrane extracellular microvesicles (MVs) from stimulated cells.[12,13] MVs are plasma membrane vesicles of 0.1-1 µm diameter released in body fluids (blood, urine, tears, etc) and in the extracellular space. One of the most solidly established feature of MVs is their procoagulant activity as a determinant of thrombosis risk in various clinical conditions, making MVs a key pathogenic markers.[14] In contrast to MVs released from the plasma membrane, exosomes, which are vesicles secreted from the membrane of inner organelles express little if any PS and are smaller in size (30 to 90 nm).[15]

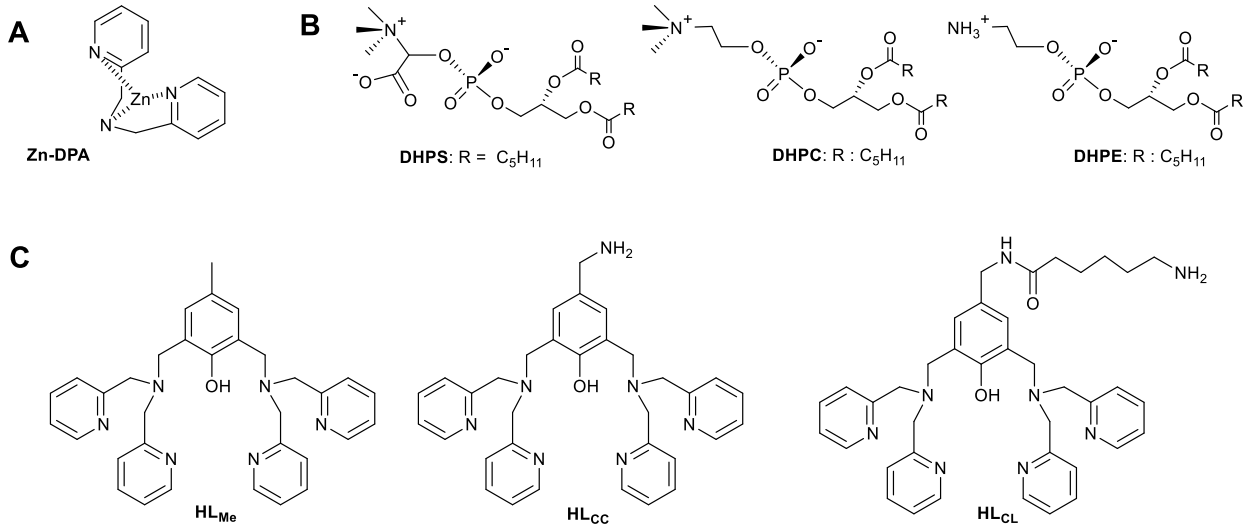

Scheme 1: Chemical structures of A) Zn- dipicolylamine (Zn-DPA) unit, B) short-chain phospholipids (DPHS:1,2-dihexanoyl-sn-glycero-3-phospho-L-serine, DHPC: 1,2-dihexanoyl-sn-glycero-3-phosphocholine, DHPE: 1,2-dihexanoyl-sn-glycero-3-phosphoethanolamine) and C) ligands used in this work

Among the current assays to measure MVs, flow cytometry has been largely used but accuracy remains challenging for particles smaller than 300 nm and is dependent on the affinity of the probes for PS.[16] For instance, the widely used PS-binding protein annexin-5, is limited by the Ca^{2+} dependence for PS binding. [17,18] Others biophysical approaches for the detection of MVs such as Nano-particle Traking Analysis (NTA) or Tunable Resistive Pulse Sensing (TRPS) directly assess the size distribution and concentration of MVs, but require specialized research laboratories and are not convenient for high throughput screening. [19] Aside from PS, MVs also convey surface identity antigens and contain biomolecules that reflect the state of the parent cell, thereby enabling the identification or their cell origin and therefore the analysis of a signature of cell activity or dysfunction in body fluids. [20] Moreover, MVs act as bioactive shuttles allowing cell cross-talk. Therefore MVs measurement in body fluids constitutes a promising tool for non-

invasive diagnosis, extensively studied in blood samples from patients with thrombotic and metabolic diseases. [21,22]

In this work, we proposed to develop an assay where MVs are directly captured by coordination complex immobilized onto a solid surface at physiological pH. Therefore the coordination compounds have to preferentially recognize PS in comparison to other zwitterionic phospholipids presented in MVs membranes such as phosphatidylcholine (PC) or phosphatidylethanolamine (PE) (Scheme1B). The choice of complexes is based on dinuclear zinc complexes developed several years ago by a team's member as models for phosphodiesterases and able to bind different phosphates anions. [23,24] Immobilization of such complexes or related variants on a solid surface was envisioned to: *1*) apply surface analysis techniques and *2*) build a simple assay for MVs detection. These inexpensive and easy-to-use synthetic coordination compounds do not present the drawbacks encountered with the use of a biological molecule, such as interference with antibodies, proteolysis or even calcium sensitivity. [18]

2. Experimental part

General information:

1,2-dihexanoyl-sn-glycero-3-phosphocholine (DHPC), 1,2-dihexanoyl-sn-glycero-3-phospho-L-serine (DHPS),1,2-dihexanoyl-sn-glycero-3-phosphoethanolamine (DHPE) and 1,2-dihexanoyl-*sn*-glycero-3-phosphate (DHPA) were obtained from Avanti Polar Lipids in powder form. N-hydrosuccinimide (NHS), 1-ethyl-3-(3-dimethylaminopropyl)carbodiimide (EDC), ethanolamine, HEPES, NaCl, Bovine Serum Albumin (BSA) (heat shock fraction, protease free, fatty acid free, essentially globulin free, pH 7, > 98 %), sodium dodecyl sulfate (SDS) and Octyl-β-Glucoside (OG) are from Sigma Aldrich. NMR spectra were recorded by using a Bruker Advance 300 (^{1}H at 300 MHz, ^{13}C at 75.5 MHz) or Bruker AV 400 (^{1}H at 400 MHz,^{13}C at 100 MHz) or AV500 (^{1}H at 500 MHz, ^{13}C at 125 MHz). ^{1}H decoupled ^{31}P NMR spectra were recorded at 298 K on a Bruker AV500 apparatus at 202.5 MHz. Chemical shifts are reported in ppm, and for ^{1}H and ^{13}C NMR

spectra, chemical shifts were referenced to the solvent signal. For ^{31}P NMR spectra, 85% phosphoric acid was used as the external reference. Spectral width, 100 ppm. ESI mass spectra were recorded on an Esquire 3000 plus Bruker Daltonics or ZQ 2000, MK II Z-spray from Waters fitted with a syringe pump. Except special notification, analysis was performed in positive mode. The working buffer (WB) used for all experiments was made of 10 mM HEPES at pH 7.4 and 150 mM NaCl in ultrapure water was filtered (0.2µm) before further used.

2.1. Synthesis:

Ligands HL_{Me} [25] and HL_{CC} [26] and complex **1** $[Zn_2(L_{Me})(\mu OH)]\cdot(ClO_4)_2]$ [23] are prepared according the procedure previously described. For ligand HL_{CL} and complex **3** $[Zn_2L_{CL}(\mu OH)]\cdot(ClO_4)_2]$ the reported syntheses [27] are improved and complex **3** and its investigations are continued.

Caution! Although no problems were encountered, suitable care and precautions should be taken when handling perchlorate salts.

Ligand HL_{CL}: N-Boc protected hexanoic acid (1.73 g, 7.47 mmol, 1.2 eq.) was dissolved with 1-[Bis(dimethylamino)methylene]-1H-1,2,3-triazolo[4,5-b]pyridinium 3-oxid hexafluorophosphate (HATU, 2.84 g, 7.5 mmol, 1.2 eq.) in CH_2Cl_2:DMF (40:10 mL) and stirred until soluble. Et_3N (2.63 mL, 18.8 mmol, 3 eq.) was added and stirred under argon with dropwise addition of the HL_{cc} (3.4 g, 6.23 mmol, 1 eq.) in 40 mL of dry CH_2Cl_2. The resulting solution was stirred two days at room temperature under argon. The solvent was evaporated and the crude oil product was re-dissolved in ethyl acetate, and washed with brine. The organic phase was dried over Na_2SO_4, filtrated and the solvent was removed under reduced pressure and purified on silica column using acetone as eluent to yield protected HL_{CL} compound as a white solid (2.96 g, 3.90 mmol, 62 % yield). *m/z*, *z* = 1, 759 $(M+H)^+$, ^1H NMR (300 MHz, $CDCl_3$), δ(ppm): 8.52 (d, 4H, *J* = 4.4 Hz, Py-o*H*), 7.61 (td, 4H, *J* = 7.7 Hz , *J* = 1.7 Hz , Py-p*H*), 7.48 (d, 4H, *J* = 7.8 Hz, Py-m'*H*), 7.12 (m, 6H), 5.83 (bs, N*H*), 5.74 (bs, N*H*), 4.32 (d, 2H, *J* = 5.4 Hz, Ar-CH_2-NH), 3.88 (s, 8H, Py-CH_2-N-), 3.82 (s, 4H, Ar-CH_2-N-), 3.08 (m, 2H, CH_2-NBoc), 2.16 (m, 2H, NH-CO-CH_2-), 1.64 (m, 2H), 1.65 (m, 2H, NH-CO-CH_2-CH_2-), 1.46-1.32 (m, 4H, -CH_2-CH_2-), 1.28 (m, 12H, *tBu*). ^{13}C NMR (75 MHz, $CDCl_3$) δ(ppm): 172.4 (Cq), 159.1 (CH), 156.0 (Cq), 155.4 (Cq), 148.9 (CH), 136.5 (CH), 129.0 (CH), 128.4 (CH), 128.0 (Cq), 124.3 (Cq), 123.0 (CH), 122.0 (CH), 59.7 (CH_2), 54.7

(CH_2), 43.4 (CH_2), 40.4 (CH_2), 36.5 (CH_2), 32.8 (CH_2), 29.8 (CH_2), 28.4 (CH_3), 26.4 (CH_2), 25.3 (CH_2).

The N-Boc protected **HL_{CL}** compound (2.9 g, 3.88 mmol, 1 eq.) is dissolved in dry CH_2Cl_2 under argon. After cooling at 0°C, 13.8 mL of trifluoroacetic acid (179 mmol, 46 eq.) in 40 mL of dry CH_2Cl_2 was added dropwise. The reaction was left to stir over night and the temperature allowed to rise to room temperature. The resulting suspension was cooled over ice, diluted with H_2O and neutralized with NaOH (2N) then NH_4OH (25%) until pH 9-10. The solution was extracted with dichloromethane and washed with brine. The organic phase was dried over Na_2SO_4, filtrated and the solvent was removed under reduced pressure to give **HL_{CL}** as a pale yellow solid (2.24 g, 3.4 mmol, 87%). ESI-MS (CH_2Cl_2): positive mode, *m/z*, *z* = 1, 659 $(M + H)^+$, 681$(M + Na)^+$; ^{1}H NMR (300 MHz, $CDCl_3$, δ ppm): 8.51 (d, 4H, *J* = 4.7 Hz, Py-o*H*), 7.57 (td, 4H, *J* = 7.6 Hz, *J* = 1.7 Hz, Py-p*H*), 7.37 (d, 4H, *J* = 7.7 Hz, Py-m'*H*), 7.12 (t, 4H, *J* = 6.5 Hz, Py-m*H*), 7.04 (s, 2H, Ar-*H*), 4.24 (d, 2H, *J* = 4.2 Hz, -C*H*$_2$-NH), 3.83 (s, 8H, Py-C*H*$_2$-N-), 3.70 (s, 4H, Ar-C*H*$_2$-N-), 2.88 (m, 2H, NH_2-C*H*$_2$), 2.24 (t, 2H, *J* = 6.8 Hz, -CO-C*H*$_2$-), 1.75 (m, 2H, NH_2-CH_2-C*H*$_2$-), 1.66 (t, 2H, *J* = 6.7 Hz, -CO-CH_2-C*H*$_2$) 1.37 (m, 2H, NH_2-$(CH_2)_2$-C*H*$_2$-). ^{13}C NMR (75 MHz, $CDCl_3$) *δ*(ppm): 172.9 (CO), 158.6 (CH), 155.0 (Cq), 148.8 (CH), 136.7 (CH), 129.5 (Cq), 128.8 (Cq), 123.7 (Cq), 123.3 (CH), 122.2 (CH), 59.9 (CH_2), 54.8 (CH_2), 42.9 (CH_2), 39.7 (CH_2), 35.6 (CH_2), 27.6 (CH_2), 25.3 (CH_2), 24.8 (CH_2). Anal. Calcd. for $C_{39}H_{46}N_8O_2$·1.85(CH_2Cl_2): C, 60.13; H, 6.14; N, 13.73. Found C, 60.16; H, 6.35; N, 13.64.

Complex 2: Ligand HL_{CC} (400 mg, 0.733 mmol, 1 eq.) was dissolved in 8 mL of acetonitrile and 215 µL (2 eq.) of Et_3N was added. A solution of $Zn(ClO_4)_2$·$6H_2O$ (0.573 g, 1.53 mmol, 2.2 eq) in acetonitrile (6 mL) was added and the mixture was stirred for 2 hours at room temperature. The solvent was partially removed under reduced pressure, then diethyl ether was added to the resulting solution and put at – 20°C overnight. The white precipitate was filtered and left to re-precipitate using acetonitrile and diethyl ether at – 20°C overnight. Finally, the precipitate was filtered to give the complex Zn_2L_{CC}µOH (280 mg, yield 43%) (**2**) as a white powder recovered in a protonated form of the following formula $[Zn_2(C_{33}H_{35}N_7O)(OH)]$·$(ClO_4)_3$ according the elemental analysis.

ESI-MS (CH_3CN) *m/z*, *z* = 2, 344.5 = $(M\text{-}2ClO_4)^{2+}$, *z* = 3, 230 = $(M\text{-}3ClO_4)^{3+}$; ^{1}H NMR (CD_3CN, 400 MHz, *δ* ppm): 3.80 (2H, s, NH_2-C*H*$_2$-), 3.82 (4H, s, Ar-C*H*$_2$-), 4.03 (4H, d, Py-C*H*$_2$-N-, *J* = 16 Hz), 3.98 (4H, d, Py-C*H*$_2$-N-, *J* = 16 Hz), 7.05 (2H, s, Ar-*H*-), 7.52 (4H, d, Py-m'*H*, *J* = 8 Hz), 7.66 (4H, t, Py-m*H*, *J* = 8.0 Hz), 8.06 (4H, t, Py-p*H*, *J* = 8.0 Hz), 8.89 (4H, d, Py-o*H*, *J* = 8 Hz).

^{13}C NMR (CD_3CN, 75 MHz, δ ppm): 48.1 (CH_2), 57.5 (CH_2), 66.3 (CH_2), 123.2 (CH), 125.9 (C_q), 126.0 (CH), 133.8 (C_q), 142.5 (CH), 149.5 (CH), 156.5 (C_q), 163.4 (CH). Anal. Calcd. for $[Zn_2(C_{33}H_{35}N_7O)(OH)]\cdot(ClO_4)_3$: C, 39.96; H, 3.66; N, 9.89. Found C, 39.90; H, 4.00; N, 9.95.

Complex 3: To a solution of HL_{CL} (0.245 g, 0.371 mmol, 1 eq.) dissolved in 15 mL of acetonitrile and with 109 µL (0.78 mmol, 2.2 eq.) of Et_3N, a solution of $Zn(ClO_4)_2{\cdot}6H_2O$ (0.290 g, 0.78 mmol, 2.2 eq) in acetonitrile (3 mL) was added and the mixture was stirred overnight at room temperature. The mixture was filtered and concentrated under reduced pressure, then diethyl ether was added and put at – 20°C for 1 week. The yellow sticky oil is re-dissolved in acetonitrile and diethyl ether was added and left again at – 20°C for 48 hours. The pale yellow precipitate is filtered and washed with diethyl ether to give as a pale yellow powder of **3** (0.166 g, yield 40 %) recovered in a protonated form of the following formula $[Zn_2(C_{33}H_{35}N_7O)(OH)]\cdot(ClO_4)_3$ according the elemental analysis. ESI-MS (CH_3CN) *m/z*, *z* = 1, 901.3 = $(M\text{-}ClO_4)^{2+}$, *z* = 2, 401.18= $(M\text{-}2ClO_4)^{2+}$; ^{1}H NMR (CD_3CN, 400 MHz, δ ppm): 1.33 (2H, m, C*H*$_2$-), 1.56 (4H, m, C*H*$_2$-), 2.14 (2H, t, CO-C*H*$_2$, *J* = 6 Hz), 2.79 (2H, t, NH_2-C*H*$_2$, *J* = 6 Hz), 3.82 (4H, s, Ar-C*H*$_2$N-), 3,99 (4H, d, Py-C*H*$_2$N-, *J* = 16 Hz), 4.03 (4H, d, Py-C*H*$_2$N-, J = 16 Hz), 4.12 (2H, d, C*H*$_2$-NH-, *J* = 4 Hz), 6.89 (1H, t, -NH-CO, *J* = 6.5 Hz), 7.51 (4H, d, Py-m*H*, *J* = 8 Hz), 7.63 (4H, d, Py-m'*H*, J = 8 Hz), 8.05 (4H, d, Py-p*H*, *J* = 8 Hz), 8.93 (4H, d, Py-o*H*, *J* = 4 Hz); ^{13}C NMR (CD_3CN, 125 MHz, δ ppm): 24.7 (CH_2), 25.1 (CH_2), 26.7 (CH_2), 35.4 (CH_2), 39.4 (CH_2), 42.9 (CH_2), 54.9 (CH_2), 60.0 (CH_2), 122.4 (CH), 123.5 (Cq), 123.6 (CH), 129.1 (Cq), 129.8 (CH), 136.9 (CH), 148.9 (CH), 155.0 (Cq), 158.4 (Cq), 173.2 (CO). Anal. Calcd. for $[Zn_2(C_{47}H_{51}N_8O_3)(OH)]\cdot(ClO_4)_3\cdot 2H_2O$: C, 45.48; H, 4.47; N, 9.03. Found C, 45.10; H, 4.18; N, 8.93

2.2. Potentiometric pH titration

The deprotonation constants of the coordinated water molecules in the complexes were determined by potentiometric p[H] titrations in a water/DMSO (70/30 by weight) solvent. The ionic strength was fixed at 0.1 M with $NaClO_4$. The measurements (at least three measurements each) were performed for each system in the pH range 5–10.5, using an automatic titrator system DMS 716 Titrino (Metrohm) with a combined glass electrode (Metrohm) filled with 3 M NaCl. The electrode was calibrated to read hydrogen ion concentration by titrating $HClO_4$ solution of known concentration with a CO_2-free NaOH solution (standardized by titrating against potassium hydrogen phtalate solution) in the water/DMSO solvent. The titrations were carried out under a

stream of argon. The GLEE program [28] was applied for the electrode calibration and check of carbonate in the NaOH solution used. The ionic product of H_2O was fixed to 14.8.[29] The potentiometric data for the titration of the complexes (0.0005 M, p[H] range 5–10.5) were refined with the HYPERQUAD program (see ESI pages 12-14), which uses non-linear least-squares fitting methods.[30] The standard deviation σ was in the range 2-4.[30]

2.3. Crystal structure determination and refinement

Measurement for $[Zn_2HL_{cc}(Cl)(H_2O)](ClO_4)_3{\cdot}2(H_2O)$ were made on a Bruker-Nonius Kappa CCD diffractometer with graphite monochromatized Mo(Kα) radiation (λ = 0.71073Å).

Crystal data for $C_{33}H_{37}ClN_7O_2Zn_2$, $3(ClO_4)$, $2(H_2O)$, Mw = 1064.27, crystal dimensions (mm): 0.49 × 0.32 × 0.15, crystal form and colour: yellow plate, crystal system: triclinic, space group : P-1, unit-cell dimensions and volume: a = 12.570(3) Å, b = 14.064(3) Å, c = 15.208(3) Å, α = 96.92(3)°, β = 113.09(3)°, γ = 113.80(3)°, V = 2135.0(10) $Å^3$, no. of formula units in the unit cell Z = 2, calculated density ρ_{calcd} = 1.656 g cm^{-3}, linear absorption coefficient μ: 1.451 mm^{-1}, temperature of measurement: T = 200 K, $2\theta_{max}$: 52°, no. of measured and independent reflections:42844 and 8367, no. of reflections with I>2σ(I): 6016, no. of parameters and restraints: 560 and 535, R_{int}: 0.0737, the final agreement factors are: R = 0.0628 and $wR2$= 0.1569 for data with I>2σ, goodness of fit S = 1.046, refinement based on F where w = $1/[\sigma^2(Fo)^2+(0.0807p)^2+6.8749p]$ where $p = (Fo^2+2Fc^2)/3$.

Determination and refinement: Data were integrated, scaled and corrected for Lorentz and polarization effects with EvalCCD software.[31] The reflections were then corrected for absorption by using the SADABS program.[32] The structures were solved by charge flipping methods then refined by full-matrix least square methods with the SHELXL program [33] implemented in Olex2 software.[34] All non-hydrogen atoms were refined with anisotropic thermal parameters. Hydrogen atoms were generated in idealized positions, riding on the carrier atoms, with isotropic thermal parameters.

CCDC 2203536 contains the full data collection parameters and structural data for $[Zn_2HL_{cc}(Cl)(H_2O)](ClO_4)_3{\cdot}2(H_2O)$. These data can be obtained free of charge from The Cambridge Crystallographic Data Centre via www.ccdc.cam.ac.uk/data request/cif

2.4. MVs isolation

MVs were isolated from human poor platelet plasma (PPP) by differential centrifugation. Pooled Normal Plasma were provided from CryoPEP (France). PPP aliquotes were rapidly thawn in a bain-marie at 37°C for 3- 4 min. Then, 1 µL of a mixture of PPACK and Dns-GGACK (50:50), protease inhibitors were added to the PPP sample to avoid clotting for 10 min at room temperature. An initial step centrifugation was done (3 min., 13 000 × g). The pellet was discarded and the supernatant underwent another centrifugation (60 min., 14 000 × g at 4°C). Supernatant was discarded again and 500 µL of working buffer (WB, 10 mM HEPES 150 mM NaCl in ultrapure water, pH 7.4, 0.2 µm filtered) was added to the pellet and vortexed for 2 min. After a final centrifugation step (60 min., 14 000 × g at 4°C), 500 µL of WB was added to the pellet. Finally, the samples were stored at 4°C and used within one week. Size distribution of MVs by TRPS showed a median size of 230 nm. The concentration of the MVs stock solution (12.5 nM eqPS) was determined as nM equivalent PS (nM eqPS) by prothrombinase assay by reference to a standard curve established using small unilamellar vesicles (DOPS:DOPC 1:2 M ratio).[35,36]

2.5. Interactions studies on solid support

Surface Plasmon Resonance (SPR) measurements were performed with a Biacore T200 (Cytiva) operated with Biacore T200 evaluation software (version 3.0.1). All measurements were performed at 25°C in WB.

A. For studies with short chain phospholipids, coordination compounds were immobilized on CM5 sensor chip (purchased from Cytivia) at 10 µL.min^{-1}. A mixture of NHS 100 mM and EDC 400 mM (50:50) was injected for 7 min on each flowcells. Coordination compounds at 250 µM in water/DMSO (70/30, v/v) solution were injected at 5µL/min on the active flowcells Then ethanolamine (1 mM) was injected 5 min at 10 µL.min^{-1} on all flowcells. The injection time of the complexes is adjusted until 1500 RU, 1250 RU or 850 RU is reached at the end of the immobilization procedure. The reference surface is obtained via a activation/desactivation procedure.

B. For studies with MVs, coordination compounds were immobilized on self-assembled monolayer exhibited carboxylate groups. Briefly, gold surfaces (FEMTO-ST institute, University

of Besançon, France) were rinsed with water, dried under nitrogen stream and exposed to UV/ozone (Jelight, Irvine, CA, USA) for 10 min. After UV/ozone treatment, the gold surface was immerged overnight in a thiol solution of HS-C_{11}-$(EG)_6$-OCH_2-COOH (1 mM), safe from light and in an environment saturated with ethanol steam. The gold surface is then washed with ethanol and blow-drying with N_2. The surface is then mounted on a sample holder and introduced in the Biacore T200 device. The complexes grafting procedure was similar to those used for CM5 sensorchip. The injection time of the complexes is adjusted until 900 RU was reached at the end of the immobilization procedure. The reference surface is obtained via a activation/desactivation procedure. BSA 3% is injected three times 120s. MVs diluted in WB supplemented with 0.03 % of BSA were injected for 720 s at a flow rate of 30 µL.min^{-1} at different concentrations and the flow-cells were rinsed with WB during 10 min. The signal recorded on the reference channel 1 was subtracted from the signal of the active channels 2, 3 and 4 to correct refractive index difference between the WB and the injected solutions.[37] The interaction with either short cbain phospholipids or MVs was not reversible, and a regeneration step composed of successive injections of SDS 0.05% 10s followed by OG 41 mM 10s was required.

3. Results and discussion

To achieve the desired grafted complexes, we chose to prepare ligands with appended amine groups on an alkyl chains introduced in *para* position of the phenol spacer (Scheme 1C). The linker length between the surface and recognition group has been reported to modulate the interaction of several biorecognition systems such as aptamer/target [38,39], peptide/protein [40] or phospholipid/protein pairs [41]. In this context, a short linker with a CH_2–NH_2 group or a longer one with a -CH_2-NHCO-$(CH_2)_5$-NH_2 group, for HL_{CC} and HL_{CL} respectively, were introduced in *para* position of the phenol spacer (Scheme 1C).The amine groups will be involved for a covalent grafting of complexes on a solid support presenting carboxylate/aldehyde groups.

3.1. Synthesis and characterization of dinuclear ligands

Introduction of an amine functionality is done through the steps described on Scheme 2. The new ligand HL_{CL}[2-((bis(pyridin-2-ylmethyl)amino)methyl)-6-((ethylamino)methyl)-4-methylaminephenol], with a potential N_6O donor set, was synthesized from HL_{CC} [26] in an overall yield of 50% (Scheme 2). Condensation of the Boc-protected hexanoic acid (**a**)[42] with HL_{CC}, followed by deprotection with TFA yielding HL_{CL} .

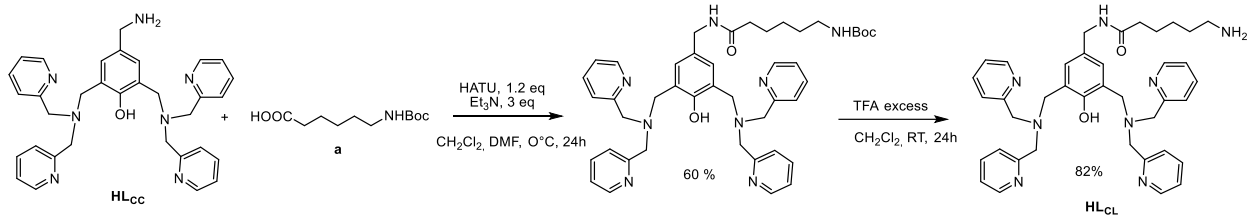

Scheme 2: Synthesis of the ligand HL_{CL}

3.2. Synthesis and characterization of dinuclear zinc complexes

Zinc complexes (Scheme 3) were prepared in acetonitrile according the same procedure.

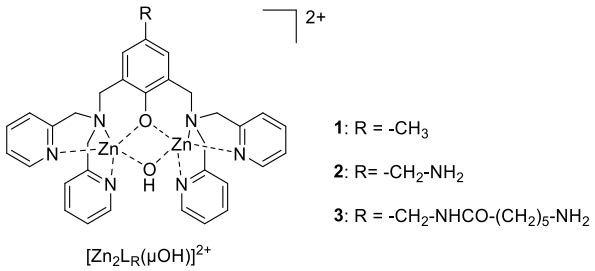

Scheme 3: Representative structure of the synthetized complexes

$Zn(ClO_4)_2.6H_2O$ was reacted with the corresponding ligands in a 2:1 M ratio in presence of two equivalents of Et_3N at ambient temperature. Pale yellow powders were isolated at -20°C after addition of THF or diethyl ether. These zinc(II) complexes were characterized in solution by ^1H NMR (Figures S3 and S5) and electrospray ionization mass spectrometry (ESI-MS) (Figures S4

and S6). The ESI-MS spectrum of **2** indicates the presence of a tri-charged species with an m/z = 230.29 (z = 3) attributed to $[M\text{-}3ClO_4^-]^{3+}$ where M corresponds to the complex with a hydroxido bridge into a phenoxido and a protonated terminal amine. A second peak with m/z =344.52 (z=2) could be assigned to $[M'\text{-}2ClO_4^-]^{2+}$ corresponding to the non-protonated terminal amine whose isotope pattern matches to $[Zn_2(C_{33}H_{35}N_7O_2)]^{2+}$ (where M' differs of M by the protonation of the terminal amine). A mono cationic species with m/z = 901.3 associated to $[Zn_2(C_{39}H_{46}N_8O_3)\text{-}ClO_4]^+$ and a di-cationic species with m/z = 401.16 associated to $[Zn_2(C_{39}H_{46}N_8O_3)\text{-}2ClO_4]^{2+}$are present in the ESI-MS spectrum of **3**. For complex **2**, the ^1H NMR spectrum is different from that of the free ligand. Almost all signals and more particularly of pyridines proton signals are slightly shifted downfield as expected upon binding to zinc ions. In the case of complex **3** (Figure S5), the pyridines proton signals are shifted downfield while the protons of the phenoxido ring are shielded from 7.08 to 6.93 ppm in a same manner as for complex **2** (from 7.19 to 7.05 ppm).

3.3 Potentiometric titrations

Complexes **2** and **3** are isolated as di-bridged forms (see complex synthesis section). In order to understand the pH behavior of these zinc complexes, we performed the protonation constant potentiometric titration. The main goal of these pK_a determination is to establish species present at physiologic pH = 7.4 used in the next part of the work. Titrations were performed in H_2O:DMSO (70:30, w:w) to ensure solubility of the complexes in the pH regions of 5-10.5. The parent complex **1** having a methyl group in place of the terminal amine groups of **2** and **3,** we can expect similar behavior in function of the pH and pK_a values in the same range. The corresponding pK_a values are listed in Table 1, and species distribution graphs are shown in Figure 1 for **2** and in ESI (Figure S7B) for **3**).

*Table 1: Value of the protonation constants determined by potentiometric titration for complexes **1-3** (0.5 mM) in H_2O:DMSO solution (70:30 by weight), I = 0.1M $NaClO_4$, T = 25 °C.*

complex	pK_{a1}	pK_{a2}
1	6.56	7.56 (*7.60*)[a]
2	6.35 ± 0.01	7.54 ± 0.08
3	6.42 ± 0.06	7.39 ± 0.01

[a] This value has been determined previously by NMR [23]

The potentiometric determined pK_{a2} values (7.54 and 7.39 from **2** and **3** respectively) mark the protonation of the bridged hydroxido in the same range as pK_{a2} value of 7.60 previously determinated by NMR [23] by us from isolated and fully characterized complexes **[**$Zn_2L_{Me}(\mu\text{-}OH)](ClO_4)_2$ (**1**) and $[Zn_2L_{Me}bis(H_2O)](ClO_4)_3$ and confirmed by potentiometric titration (pK_{a2} = 7.56) in this work. This value is in line with those founded in literature for di-bridged phenoxido, hydroxido complexes with pK_a = 7.4 ± 0.1 [43]; 7.11 [44] or from series of dinuclear zinc complexes based on pyrazole spacer displaying pK_a values for the bridging hydroxido from 7.57 to 8.04. [45,46] Regarding the attribution of pK_{a1} (6.35 and 6.42 from **2** and **3** respectively) a preliminary titration by ^{1}H NMR of ligand HL_{CC} as function of pD (pD = pH + 0.4) [47] (Figure S8) shows significant chemical shift variations for pyridyl and methylene protons close to pyridyl or tertiary amine groups at pH ≤ 7. After zinc complexation, all groups are potentially deprotonated in the same range, including the phenolic proton not observable in aqueous solution. In litterature previous studies on bridged phenoxido dinuclear zinc complexes display deprotonation of the phenolic group (pK_{Ph} = 6.97 ± 0.05)[43] and agree with others reported constants for the deprotonation of M(II)-bound phenol [48]. However, we cannot rule out the involment of a pyridyl

or tertiary amine in pK_{a1} rending an unambiguously identification not possible. Deprotonation of the terminal amine groups of the anchoring arms requires higher pH as observed on NMR titration of HL_{CC} (Figure S8). A proposal for the main protonation equilibria observed for complexes **2**-**3** is shown on Scheme 4.

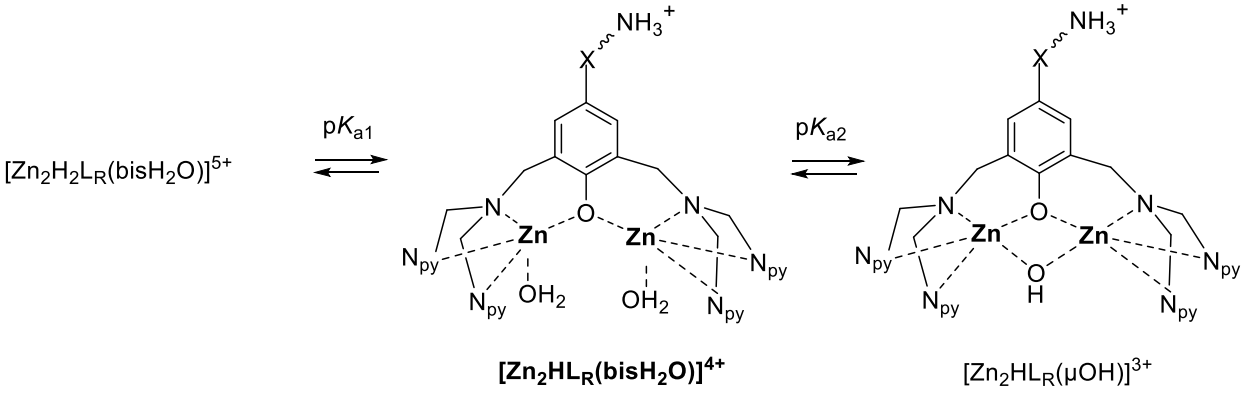

Scheme 4. Proposed species and equilibria in H_2O:DMSO (70:30). The structure in bold represent the main species at physiologic pH = 7.4

This study evidences that complexes **2** and **3** are subject to pH driven changes and the most interesting result is that around pH =7.4 (the physiologic pH used in the next part of the work) the predominant forms are the mono-phenoxido bridged species with aquo-pendant ligands according to the RX structure obtained from **1** in aqueous medium. [23]

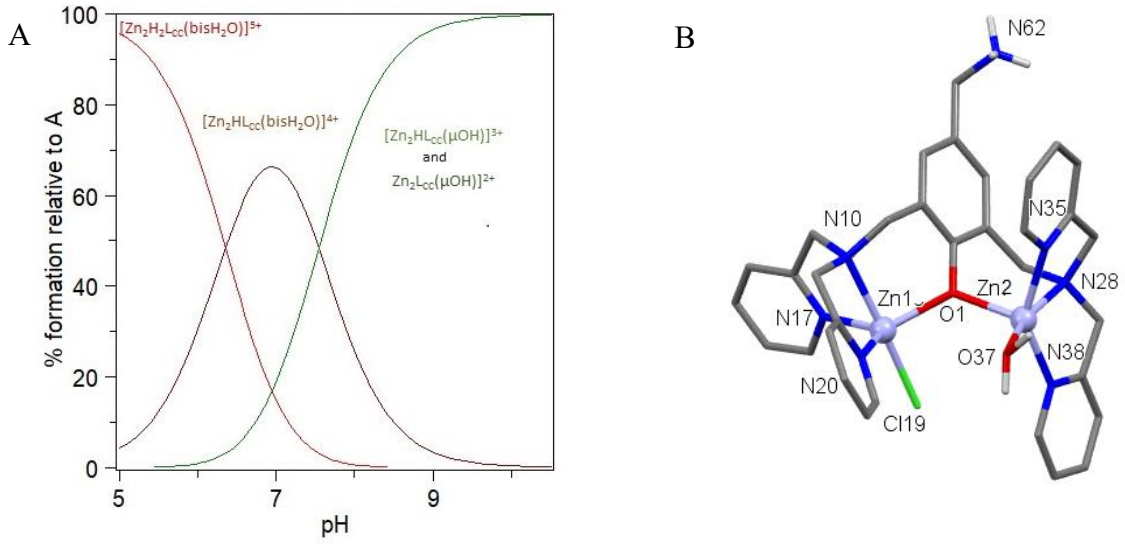

*Figure 1: For complex **2**: (A) species distribution in H_2O:DMSO (70:30), $[Zn_2HL_{CC}(\mu OH)]^{3+}$ and $[Zn_2HL_{CC}(\mu OH)]^{2+}$ represent cationic part of complex **1** with the terminal amine protonated and non protonated*; *(B) X-ray structure of $[Zn_2HL_{CC}(Cl)(H_2O)](ClO_4)_3$ 2(H_2O) obtained by slow evaporation in aqueous solution. H atoms (except for the aquo and terminal amine group) and the ClO_4^- counteranions were omitted for clarity (selected bond lengths and bond angles are in ESI, Tables S1 and S2.*

3.4 X-Ray

To confirm the presence of the expected species, crystallization batches were made of **2** and **3**. Slow evaporation (months) of an aqueous solution of **2** at room temperature resulted in pale yellow crystals suitable for X-ray analysis (details in the experimental section). As shown in Figure 1B, the X-ray structure obtained reveals that the two zinc atoms are mono-bridged by the oxygen atom of the phenoxido spacer and lie on opposite sides of the phenoxido ring plane. The pentacoordination of Zn1 and Zn2 is completed for each by the tertiary amine, two pyridine nitrogen atoms and one exchangeable ligand. As one exchangeable ligand is an exogeneous chlorine for Zn1 (potentially from degradation of the perchlorate counteranion) and the other an aquoligand for Zn2, the complex exhibits dissymmetry. The coordination polyhedron around Zn1 is a distorted trigonal bipyramid (τ parameter equal to 0.9) whose axial positions are occupied by

the tertiary nitrogen atom and the chlorine. The coordination environment around Zn2 forms a distorted square pyramid (τ parameter equal to 0.3) with the tertiary amine and the aquoligand in axial positions. The intermetallic distance Zn1…Zn2 is 3.649 Å shorter than the distance of 3.791Å of the relevant complex $[Zn_2L_{Me}bis(H_2O)](ClO_4)_3$ previously characterized.[23] The presence of three perchlorates counteranion is consistent with the protonation of the terminal amine.

3.5 Binding studies

3.5.1 In solution: ^{31}P NMR

In a preliminary approach, the interaction between zinc complex **3** and model phospholipids in solution have been studied by the analysis of the changes induced on the ^{31}P NMR. The short-chain phospholipids monomers used are DHPS (1,2-dihexanoyl-sn-glycero-3-phospho-L-serine) and DHPC (1,2-dihexanoyl-sn-glycero-3-phosphocholine) which are analogous of phosphatidylserine and phosphatidylcholine, respectively, but whose hydrophobic part has only 6 carbons (Figure 2A-B). This allows their solubilization in aqueous medium and at the concentrations used (5 mM) to be in the form of monomers below their critical micellar concentration (CMC ~ 15 mM for DHPC and 8 mM for DHPS in 50 mM Tris, 175 mM NaCl, pH 7.4) [49] which allows a study of interactions at the molecular level. The free DHPC shows a distinguishable signal at δ= 1.005 ppm. In the presence of complex **3** (1 eq.), this signal is invariant (Figure 2A).

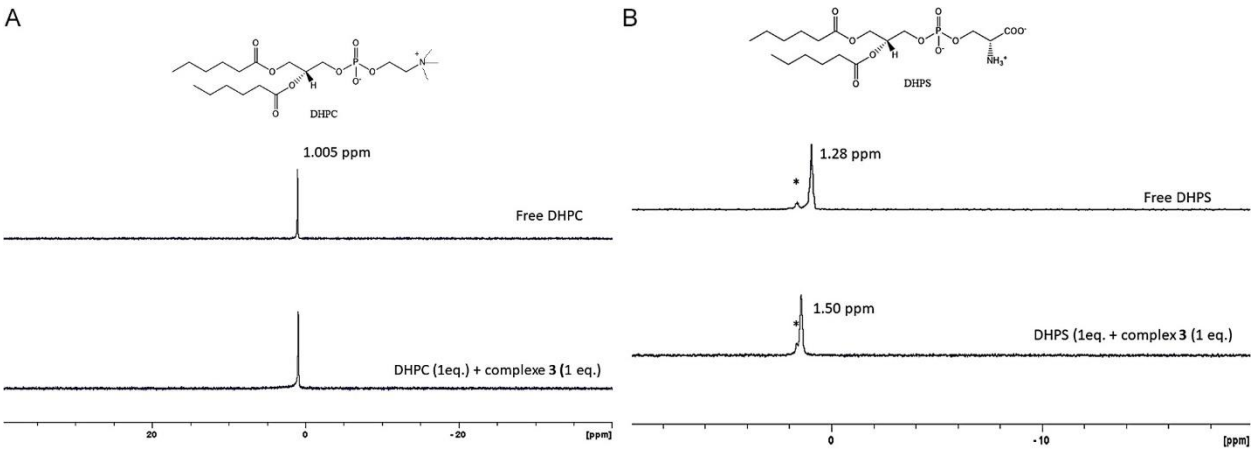

*Figure 2. ^{1}H-decoupled ^{31}P NMR spectra in HEPES solution buffered at 7.4 pH:DMSO (70:30) at 25°C for: A) (top) DHPC at 5 mM, (down) DHPC + complex **3** (1 eq.) and B): (top) DHPS at 5 mM, (down) DHPS + complex **3** (1 eq.). * represent an impurity present in the sample*

The spectrum of free DHPS displays one signal at δ =1.28 ppm. The presence of one eq. of complex **3** induced a slight shift (δ = 1.50) in a unique signal that provided evidence of the fast exchange at the NMR time scale (Figure 2B). These data suggest that, in these experimental conditions, the anionic DHPS could interact with the cationic complex in contrast to the zwitterionic DHPC. The negative charge of DHPS due to the carboxylate group close to the phosphate one could be the cause of this difference in recognition between DHPS and DHPC. Further insights for interaction studies can be obtained in supported phase (see below).

3.5.2 Surface Plasmon (SPR) measurement.

The ability to available zinc complexes to capture MVs was evaluated on supported phase using surface plasmon resonance (SPR) for real-time, label-free detection. [50,51] The amine group added to complexes **2** and **3** on their grafting arm (Figure 1C) allowed covalent coupling to sensor CM5 chips having carboxylate groups. As a first step, short-chain phospholipids were evaluated in order to confirm that DHPS recognition still occurs after immobilization of the complexes. Phospholipids with short aliphatic chains have been selected to study interactions at the molecular

level. Indeed, reduction of the aliphatic chains of phospholipids allows their solubilization in aqueous media as monomers while working below their critical micellar concentration.[49] Raw signal recorded upon injection of DHPS solutions on the reference surface have squared profiles (black line in Figure S9) confirming the absence of nonspecific interactions. In contrast, curved profiles with significant increase of the response are recorded on surfaces modified by complexes (red line in Figure S9) that demonstrated the interaction of DHPS with the two zinc complexes immobilized on surfaces. It is noteworthy that the SPR signals do not decrease upon the dissociation step. The interaction with DHPS is almost irreversible and a regeneration step was required after injection of each DHPS solution. Double-substracted sensorgrams recorded upon injection of short-chain phospholipids at 750 μM on immobilized complexes **3** are represented on Figure 3A. Interestingly, in contrast to DHPS, signal variations are not observed upon injections of either DHPE or DHPC (Scheme 1B). These results suggested that zinc complexes interact specifically with DHPS in comparison to other zwitterionic phospholipids such as DHPE or DHPC.

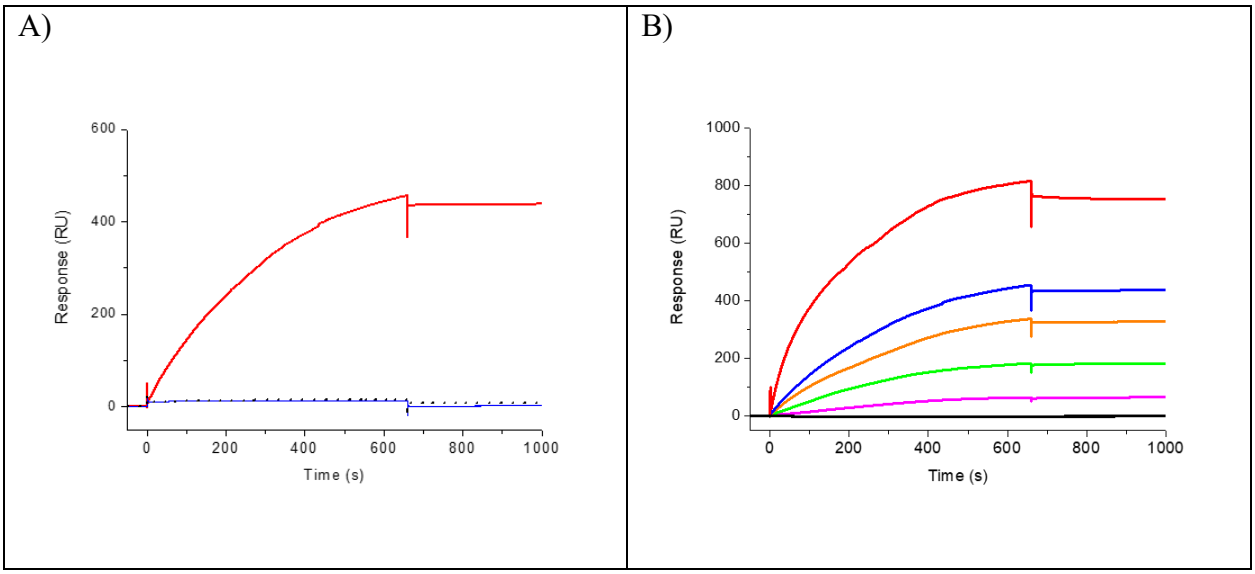

*Figure 3. Sensorgrams recorded on surface modified by complex **3** (1500 RU) upon A) injection of 750 µM solution of DHPS (red), DHPC (black) and DHPE (blue); B) injection of DHPS solution at 100 µM, 250 µM, 500µM, 750 µM, and 1500µM (curves from bottom to top).*

Injections of DHPS at concentrations ranging from 100 µM to 1500 µM led to an increase in the SPR response (Figure 3B and Figure S11). However, the equilibrium thermodynamic constant could not be accurately determined upon these experimental conditions as equilibrium is not reached at the end of the association phase (Figure 3B). The reduction in the level of immobilization of the complexes on the surface led to biphasic curves (Figure S10) probably linked to potential electrostatic repulsion between DHPS and residual carboxylate groups of dextran matrix. [52] Nevertheless, the specific recognition of DHPS in comparison to DHPE and DHPC was also confirmed for grafted surfaces with lower levels of immobilization of the complexes (Figure S10A). Similar results are obtained on surfaces fonctionnalized with complex **2** (Figure S10B). Interestingly, sensorgrams recorded upon injection of DHPA (Figures S10A and S10C) demonstrated that both complexes can interact with the phosphate group of DHPA that is fully accessible for coordination. Taking together, these latter results suggested that recognition of

DHPS by complexes **2** and **3** is impacted by the chemical groups (i.e the carboxylate) close to the phosphate, which provide a negative charge, resulting in an enhanced interaction.

Of particular interest is that additional SPR experiments were performed using MVs isolated from human plasma by sequential centrifugation and characterized by two different assays (prothrombinase assay and TRPS). MVs detach from the plasma membrane of cells that expose PS on their surface and thus have a promising diagnostic value. Therefore, we evaluated the capture of MVs by the zinc compounds based on PS/complex interactions. To perform these experiments, we used a carboxy-terminated self-assembled monolayer (SAM) prepared on a gold surface using bifunctional PEGylated alkanethiols. After amine coupling of the complexes, passivation of the surface by injection of BSA and WB supplemented with 0.05% BSA were used to limit non-specific binding of MVs. Double subtracted sensorgrams recorded upon injection of MVs on surface modified by complex **3** are shown on Figure 4A. It should be noted that MVs concentration are expressed in nM eqPS as they are quantified using a prothrombinase assay. [35,36]

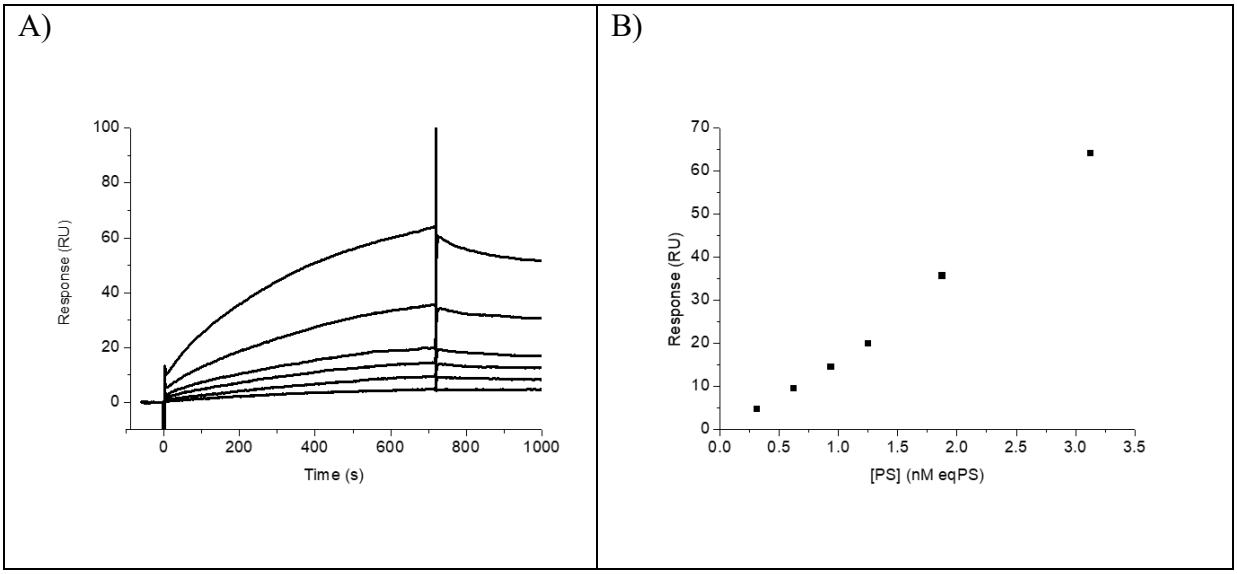

*Figure 4. A) Sensorgrams recorded for injection of MVs at concentrations 0.31, 0.62, 0.94, 1.88 and 3.13 nM eqPS (curves from bottom to top) on surface modified by complex **3** and B) response at the end of the association phase as a function of MVs concentration (determined by prothrombinase assay, square).*

The sensorgram profiles obtained confirmed the interaction between the MVs and the zinc complexes. A slight dissociation of the MVs from the surface is observed when rinsing with buffer. The response at the end of the association phase increases with the concentration of injected MVs (Figure 4B for complex **3** and Figure S12 for complex **2**). The short and long linkers appear to allow accessibility of the metal core for interaction with the PS exposed to the MVs membrane (Figure S12). These results indicate that zinc compounds **2** and **3** are capable of capturing MVs on the surface through their selective recognition of PS and thus pave the way for the use of zinc complexes in assays for further characterization of MVs.

4. Conclusion

Two new zinc dinuclear complexes (**2** and **3**) containing *1*) a phenoxido bridge and a hydroxido bridge, and *2*) an amine group appended to an alkyl chain were prepared and characterized. The alkyl-amine group (a short CH_2-NH_2 group or a longer CH_2-NHCO-$(CH_2)_5$-NH_2 group) was introduced in the para position of the phenoxido spacer for covalent grafting onto a solid support. Potentiometric titration in a mixed H_2O/DMSO medium evidence that **2** and **3** exhibit similar behavior. Both undergo pH-driven interconversion in accordance with the relevant complex **1** (without an amine arm for anchoring) previously reported. **[23]** At physiologic pH, the main species have two aquo-pendant ligands in place of the μ-OH bridge. The obtained X-ray structure corroborates the structural hypotheses for conversion of **2** in a mono-phenoxido bridged species in aqueous neutral medium. As a starting point for phospholipid interactions studies, ^{31}P NMR was used in solution with DHPS and DHPC. From the signal of DHPC, no changes have been detected in presence of **2** while a modification of the DHPS signal was observed in the presence of **2** (1:1). PS recognition was evaluated using SPR after complexes immobilization on solid supports. Results

confirmed the selective recognition of complexes **2** and **3** for DHPS as compared to DHPC and DHPE. Immobilization using both spacer lengths enables DHPS/complexes recognition in the present experimental conditions. Moreover, both complexes have also demonstrated their ability to capture MVs isolated from human plasma. These results highlight that zinc coordination assemblies described herein at physiological pH = 7.4, display appropriate charge, geometry, bridging unit, metal-metal distances and spatial orientation to preferentially bind anionic phospholipids (PS) over zwitterionic phospholipids (PC or PE). These features can be at the origin of the selective recognition observed in this work including MVs extracted from biological samples. These complexes are without any doubt promising candidates for MVs probing by a new approach based on coordination chemistry.

5. Acknowledgements

The authors gratefully acknowledge the French Research Agency for financial support (ANR-16-CE29-0009) and a grant for PC, and to ICMG UAR 2607 (PCN-ICMG) for the analytical facilities (NMR, ESI-MS, X-Ray and SPR). This work has been partially supported by the CBH-EUR-GS (ANR-17-EURE-003) program and the Labex Arcane (ANR-11-LABX-0003-01) in the framework of which this work was carried out.

6. References

[1] H.T. Ngo, X. Liu, K.A. Jolliffe, Anion recognition and sensing with Zn(ii)–dipicolylamine complexes, Chem. Soc. Rev. 41 (2012) 4928–4965. https://doi.org/10.1039/C2CS35087D.

[2] J.A. Drewry, P.T. Gunning, Recent advances in biosensory and medicinal therapeutic applications of zinc(II) and copper(II) coordination complexes, Coord. Chem. Rev. 255 (2011) 459–472. https://doi.org/10.1016/j.ccr.2010.10.018.

[3] A. Zachowski, Phospholipids in animal eukaryotic membranes: transverse asymmetry and movement, Biochem J. 294 (1993) 1–14. https://doi.org/10.1042/bj2940001.

[4] E.J. O'Neil, B.D. Smith, Anion recognition using dimetallic coordination complexes, Coord. Chem. Rev. 250 (2006) 3068–3080. https://doi.org/10.1016/j.ccr.2006.04.006.

[5] E.J. O'Neil, H. Jiang, B.D. Smith, Effect of bridging anions on the structure and stability of phenoxide bridged zinc dipicolylamine coordination complexes, Supramol. Chem. 25 (2013) 315–322. https://doi.org/10.1080/10610278.2013.776170.
[6] N. Kumar, Roopa, V. Bhalla, M. Kumar, Beyond zinc coordination: Bioimaging applications of Zn(II)-complexes, Coord. Chem. Rev. 427 (2021) 213550. https://doi.org/10.1016/j.ccr.2020.213550.
[7] K.J. Clear, K.M. Harmatys, D.R. Rice, W.R. Wolter, M.A. Suckow, Y. Wang, M. Rusckowski, B.D. Smith, Phenoxide-Bridged Zinc(II)-Bis(dipicolylamine) Probes for Molecular Imaging of Cell Death, Bioconjug. Chem. 27 (2016) 363–375. https://doi.org/10.1021/acs.bioconjchem.5b00447.
[8] V.E. Zwicker, B.L. Oliveira, J.H. Yeo, S.T. Fraser, G.J.L. Bernardes, E.J. New, K.A. Jolliffe, A Fluorogenic Probe for Cell Surface Phosphatidylserine Using an Intramolecular Indicator Displacement Sensing Mechanism, Angew. Chem. Int. Ed. 58 (2019) 3087–3091. https://doi.org/10.1002/anie.201812489.
[9] D.R. Rice, K.J. Clear, B.D. Smith, Imaging and therapeutic applications of zinc(II)-dipicolylamine molecular probes for anionic biomembranes, Chem. Commun. 52 (2016) 8787–8801. https://doi.org/10.1039/C6CC03669D.
[10] P. Ashokkumar, A.H. Ashoka, M. Collot, A. Das, A.S. Klymchenko, A fluorogenic BODIPY molecular rotor as an apoptosis marker, Chem. Commun. 55 (2019) 6902–6905. https://doi.org/10.1039/C9CC03242H.
[11] B.A. Smith, W.J. Akers, W.M. Leevy, A.J. Lampkins, S. Xiao, W. Wolter, M.A. Suckow, S. Achilefu, B.D. Smith, Optical Imaging of Mammary and Prostate Tumors in Living Animals using a Synthetic Near Infrared Zinc(II)-Dipicolylamine Probe for Anionic Cell Surfaces, J. Am. Chem. Soc. 132 (2010) 67–69. https://doi.org/10.1021/ja908467y.
[12] L. Doeuvre, L. Plawinski, F. Toti, E. Anglés-Cano, Cell-derived microparticles: a new challenge in neuroscience, J. Neurochem. 110 (2009) 457–468. https://doi.org/10.1111/j.1471-4159.2009.06163.x.
[13] A.E. Sedgwick, C. D'Souza-Schorey, The biology of extracellular microvesicles, Traffic. 19 (2018) 319–327. https://doi.org/10.1111/tra.12558.
[14] C. Voukalis, E. Shantsila, G.Y.H. Lip, Microparticles and cardiovascular diseases, Ann. Med. 51 (2019) 193–223. https://doi.org/10.1080/07853890.2019.1609076.
[15] M.Z. Ratajczak, J. Ratajczak, Extracellular microvesicles/exosomes: discovery, disbelief, acceptance, and the future?, Leukemia. 34 (2020) 3126–3135. https://doi.org/10.1038/s41375-020-01041-z.
[16] C. Gardiner, D.D. Vizio, S. Sahoo, C. Théry, K.W. Witwer, M. Wauben, A.F. Hill, Techniques used for the isolation and characterization of extracellular vesicles: results of a worldwide survey, J. Extracell. Vesicles. 5 (2016) 32945. https://doi.org/10.3402/jev.v5.32945.
[17] Y.-H. Ma, B. Li, J. Yang, X. Han, Z. Chen, X. Lu, Calcium-dependent and -independent annexin V binding: distinct molecular behaviours at cell membrane interfaces, Chem Comm. 56 (2020) 1653–1656. https://doi.org/10.1039/C9CC09184J.
[18] W. van Heerde, Markers of apoptosis in cardiovascular tissues focus on Annexin V, Cardiovasc Res. 45 (2000) 549–559. https://doi.org/10.1016/S0008-6363(99)00396-X.
[19] S.M. Davidson, C.M. Boulanger, E. Aikawa, L. Badimon, L. Barile, C.J. Binder, A. Brisson, E. Buzas, C. Emanueli, F. Jansen, M. Katsur, R. Lacroix, S.K. Lim, N. Mackman, M. Mayr, P. Menasché, R. Nieuwland, S. Sahoo, K. Takov, T. Thum, P. Vader, M.H.M. Wauben, K.

Witwer, J.P.G. Sluijter, Methods for the identification and characterization of extracellular vesicles in cardiovascular studies: from exosomes to microvesicles, Cardiovasc. Res. (2022) cvac031. https://doi.org/10.1093/cvr/cvac031.
[20] O. Morel, F. Toti, B. Hugel, J.-M. Freyssinet, Cellular microparticles: a disseminated storage pool of bioactive vascular effectors:, Curr. Opin. Hematol. 11 (2004) 156–164. https://doi.org/10.1097/01.moh.0000131441.10020.87.
[21] S.F. Mause, C. Weber, Microparticles: Protagonists of a Novel Communication Network for Intercellular Information Exchange, Circ. Res. 107 (2010) 1047–1057. https://doi.org/10.1161/CIRCRESAHA.110.226456.
[22] X. Delabranche, J.-P. Quenot, T. Lavigne, E. Mercier, B. François, F. Severac, L. Grunebaum, M. Mehdi, F. Zobairi, F. Toti, F. Meziani, J. Boisramé-Helms, Early Detection of Disseminated Intravascular Coagulation During Septic Shock: A Multicenter Prospective Study, Crit. Care Med. 44 (2016) e930–e939. https://doi.org/10.1097/CCM.0000000000001836.
[23] K. Selmeczi, C. Michel, A. Milet, I. Gautier-Luneau, C. Philouze, J.-L. Pierre, D. Schnieders, A. Rompel, C. Belle, Structural, Kinetic, and Theoretical Studies on Models of the Zinc-Containing Phosphodiesterase Active Center: Medium-Dependent Reaction Mechanisms, Chem. - Eur. J. 13 (2007) 9093–9106. https://doi.org/10.1002/chem.200700104.
[24] C. Belle, I. Gautier-Luneau, L. Karmazin, J.-L. Pierre, S. Albedyhl, B. Krebs, M. Bonin, Regio-Directed Synthesis of a ZnIIFeIII Complex from an Unsymmetrical Ligand and Its Relevance to Purple Acid Phosphatases, Eur. J. Inorg. Chem. 2002 (2002) 3087–3090. https://doi.org/10.1002/1099-0682(200212)2002:12<3087::AID-EJIC3087>3.0.CO;2-0.
[25] S. Torelli, C. Belle, I. Gautier-Luneau, J.L. Pierre, E. Saint-Aman, J.M. Latour, L. Le Pape, D. Luneau, pH-Controlled Change of the Metal Coordination in a Dicopper(II) Complex of the Ligand H−BPMP: Crystal Structures, Magnetic Properties, and Catecholase Activity, Inorg. Chem. 39 (2000) 3526–3536. https://doi.org/10.1021/ic991450z.
[26] S. Gentil, J.K. Molloy, M. Carrière, A. Hobballah, A. Dutta, S. Cosnier, W.J. Shaw, G. Gellon, C. Belle, V. Artero, F. Thomas, A. Le Goff, A Nanotube-Supported Dicopper Complex Enhances Pt-free Molecular H2/Air Fuel Cells, Joule. 3 (2019) 2020–2029. https://doi.org/10.1016/j.joule.2019.07.001.
[27] C. Belle, G. Gellon, L. Plawinski, L. Doeuvre, E. Angles Cano, Grafted dinuclear metal complexes and use thereof as cellular microparticle sensors, PCT/FR2012/050610, n.d.
[28] P. Gans, GLEE, a new computer program for glass electrode calibration, Talanta. 51 (2000) 33–37. https://doi.org/10.1016/S0039-9140(99)00245-3.
[29] J.-C. Hallé, R. Gaboriau, Etude électrochimique des mélanges d'eau et de diméthylsulfoxide. Produit ionique apparent et niveau d'acidité, Bull Soc Chim. (1966) 1851–1857.
[30] P. Gans, A. Sabatini, A. Vacca, Investigation of equilibria in solution. Determination of equilibrium constants with the HYPERQUAD suite of programs, Talanta. 43 (1996) 1739–1753. https://doi.org/10.1016/0039-9140(96)01958-3.
[31] A.J.M. Duisenberg, L.M.J. Kroon-Batenburg, A.M.M. Schreurs, An intensity evaluation method: *EVAL* -14, J. Appl. Crystallogr. 36 (2003) 220–229. https://doi.org/10.1107/S0021889802022628.
[32] SADABS-2004/1, Program for empirical absorption correction of area detector data, Univerty of Gottingen, Germany, 2003.

[33] G.M. Sheldrick, A short history of SHELX, Acta Crystallogr. A. 64 (2008) 112–122. https://doi.org/10.1107/S0108767307043930.
[34] O.V. Dolomanov, L.J. Bourhis, R.J. Gildea, J.A.K. Howard, H. Puschmann, OLEX2 : a complete structure solution, refinement and analysis program, J Appl Cryst. 42 (2009) 339–341. https://doi.org/10.1107/S0021889808042726.
[35] I.M. Bugueno, F. Zobairi El-Ghazouani, F. Batool, H. El Itawi, E. Anglès-Cano, N. Benkirane-Jessel, F. Toti, O. Huck, Porphyromonas gingivalis triggers the shedding of inflammatory endothelial microvesicles that act as autocrine effectors of endothelial dysfunction, Sci. Rep. 10 (2020) 1778. https://doi.org/10.1038/s41598-020-58374-z.
[36] B. Hugel, F. Zobairi, J.-M. Freyssinet, Measuring circulating cell-derived microparticles, J Thromb Haemost. 2 (2004) 1846–1847. https://doi.org/10.1111/j.1538-7836.2004.00936.x.
[37] R. Rich, Advances in surface plasmon resonance biosensor analysis, Curr Opin Biotechnol. 11 (2000) 54–61. https://doi.org/10.1016/S0958-1669(99)00054-3.
[38] J.A. Martin, Y. Chushak, J.L. Chávez, J.A. Hagen, N. Kelley-Loughnane, Microarrays as Model Biosensor Platforms to Investigate the Structure and Affinity of Aptamers, J Nucleic Acids. 2016 (2016) 1–11. https://doi.org/10.1155/2016/9718612.
[39] M. Pons, M. Perenon, H. Bonnet, E. Gillon, C. Vallée, L. Coche-Guérente, E. Defrancq, N. Spinelli, A. Van der Heyden, J. Dejeu, Conformational transition in SPR experiments: impact of spacer length, immobilization mode and aptamer density on signal sign and amplitude, The Analyst. (2022) 10.1039.D2AN00824F. https://doi.org/10.1039/D2AN00824F.
[40] A. Imran, B.S. Moyer, A.J. Wolfe, M.S. Cosgrove, D.E. Makarov, L. Movileanu, Interplay of Affinity and Surface Tethering in Protein Recognition, J Phys Chem Lett. 13 (2022) 4021–4028. https://doi.org/10.1021/acs.jpclett.2c00621.
[41] H.L. Birchenough, M.J. Swann, E. Zindy, A.J. Day, T.A. Jowitt, Enhanced avidin binding to lipid bilayers using PDP-PE lipids with PEG-biotin linkers, Nanoscale Adv. 2 (2020) 1625–1633. https://doi.org/10.1039/D0NA00060D.
[42] M.B. Doughty, C.S. Chaurasia, K. Li, Benextramine-neuropeptide Y receptor interactions: contribution of the benzylic moieties to [3H]neuropeptide Y displacement activity, J. Med. Chem. 36 (1993) 272–279. https://doi.org/10.1021/jm00054a012.
[43] N.V. Kaminskaia, B. Spingler, S.J. Lippard, Hydrolysis of β-Lactam Antibiotics Catalyzed by Dinuclear Zinc(II) Complexes: Functional Mimics of Metallo-β-lactamases, J. Am. Chem. Soc. 122 (2000) 6411–6422. https://doi.org/10.1021/ja993704l.
[44] C. Pathak, D. Kumar, M.K. Gangwar, D. Mhatre, T. Roisnel, P. Ghosh, Heterodinuclear Zn(II)−Fe(III) and Homodinuclear M(II)−M(II) [M = Zn and Ni] complexes of a Bicompartmental [N 6 O] ligand as synthetic mimics of the hydrolase family of enzymes, J. Inorg. Biochem. 185 (2018) 30–42. https://doi.org/10.1016/j.jinorgbio.2018.04.018.
[45] L.R. Gahan, S.J. Smith, A. Neves, G. Schenk, Phosphate Ester Hydrolysis: Metal Complexes As Purple Acid Phosphatase and Phosphotriesterase Analogues, Eur. J. Inorg. Chem. 2009 (2009) 2745–2758. https://doi.org/10.1002/ejic.200900231.
[46] K.E. Dalle, F. Meyer, Modelling Binuclear Metallobiosites: Insights from Pyrazole-Supported Biomimetic and Bioinspired Complexes, Eur. J. Inorg. Chem. 2015 (2015) 3391–3405. https://doi.org/10.1002/ejic.201500185.
[47] P.K. Glasoe, F.A. Long, Use of Glass Electrodes to Measure Acidities in Deuteriem Oxide, J. Phys. Chem. 64 (1960) 188–190. https://doi.org/10.1021/j100830a521.

[48] E. Kimura, T. Koike, K. Uenishi, M. Hediger, M. Kuramoto, S. Joko, Y. Arai, M. Kodama, Y. Iitaka, New-dimensional cyclam. Synthesis, crystal structure, and chemical properties of macrocyclic tetraamines bearing a phenol pendant, Inorg. Chem. 26 (1987) 2975–2983. https://doi.org/10.1021/ic00265a012.

[49] V. Koppaka, J. Wang, M. Banerjee, B.R. Lentz, Soluble Phospholipids Enhance Factor X_a -Catalyzed Prothrombin Activation in Solution, Biochemistry. 35 (1996) 7482–7491. https://doi.org/10.1021/bi952063d.

[50] E.L. Gool, I. Stojanovic, R.B.M. Schasfoort, A. Sturk, T.G. van Leeuwen, R. Nieuwland, L.W.M.M. Terstappen, F.A.W. Coumans, Surface Plasmon Resonance is an Analytically Sensitive Method for Antigen Profiling of Extracellular Vesicles, Clin. Chem. 63 (2017) 1633–1641. https://doi.org/10.1373/clinchem.2016.271049.

[51] S. Obeid, A. Ceroi, G. Mourey, P. Saas, C. Elie-Caille, W. Boireau, Development of a NanoBioAnalytical platform for “on-chip” qualification and quantification of platelet-derived microparticles, Biosens. Bioelectron. 93 (2017) 250–259. https://doi.org/10.1016/j.bios.2016.08.100.

[52] R.B.M. Schasfoort, A.J. Tudos, eds., Handbook of Surface Plasmon Resonance:, Royal Society of Chemistry, Cambridge, 2008. https://doi.org/10.1039/9781847558220.